Int. J. Electrochem. Sci., 8 **(2013)** 2023 - 2033

International Journal of
ELECTROCHEMICAL
SCIENCE
www.electrochemsci.org

Candesartan Cilexetil Determination by Electrode Modified with Hybrid Film of Ionic Liquid- Graphene Nanosheets-Silicon Carbide Nanoparticle Using Continuous Coulometric FFT Cyclic Voltammetry

P. Norouzi[1,*], *M. Pirali-Hamedani*,[2,3]*M. R. Ganjali*[1]

[1]Center of Excellence in Electrochemistry, University of Tehran, Tehran, Iran
[2] Department of Medicinal Chemistry, Faculty of Pharmacy, Tehran University of Medical Sciences, Tehran, Iran
[3] Pharmaceutical Sciences Research Center, Tehran, Iran
[*]E-mail: norouzi@khayam.ut.ac.ir

Received: 30 November 2012 / *Accepted:* 6 January 2013 / *Published:* 1 February 2013

In this work, a new electrochemical method is introduced for the determination of Candesartan cilexetil using a new sensor and Continuous Coulometric Fast Fourier transformation cyclic voltammetry (CCFFTCV). The new sensor was designed based on silicon carbide nanoparticles and graphene nanosheets hybrid mixed with ionic liquid (1-Butyl-3-methylimidazolium hexafluorophosphate ([bmim][PF_6]) on a glassy carbon electrode. The sensor response calculated in form of coulomb by integrating the charge changes under the peak current in a selected potential range. The experimental conditions, for the electrochemical measurement were optimized. The linear concentrations range of Candesartan cilexetil was from 0.5 to 120×10^{-8} M with a detection limit of 5.2×10^{-9} M. Moreover, the proposed sensor exhibits good accuracy, the response time less than 6s, high sensitivity with repeatability (R.S.D value of 3.5%) and long term stability, 55 days with a decrease of 2.3% in the response.

Keywords: FFT cyclic Voltammetry; Candesartan cilexetil; Silicon carbide nanoparticles; Graphene nanosheets; Ionic liquid

1. INTRODUCTION

Angiotensin converting enzyme (ACE) inhibitors are still considered first-line therapy in heart failure [1]. Angiotensin II-receptor antagonists are an alternative to the more traditional ACE inhibitors and may offer further benefits compared with ACE inhibitors [1-3]. Candesartan cilexetil (2-ethoxy-1-({4-[2-(2H-1,2,3,4-tetrazol-5-yl)phenyl]phenyl}methyl)-1H-1,3-benzodiazole-6-carboxylic acid)

(scheme 1) is a potent and selective angiotensin II type 1 receptor blocker, which has widely been used orally in patients with hypertension, heart failure, and kidney disease [4,5].

Various analytical methods have been applied for determination of Candesartan cilexetil (CAC) in pharmaceutical formulations and biological fluids, including HPLC with fluorometric detection [6], HPLC–MS [7], SPE-LC–MS [8] spectrophotometric [9] and voltammetric method [10]. All these methods are very tedious, time consuming and involve complex procedures, therefore require expensive instruments and skilled individuals.

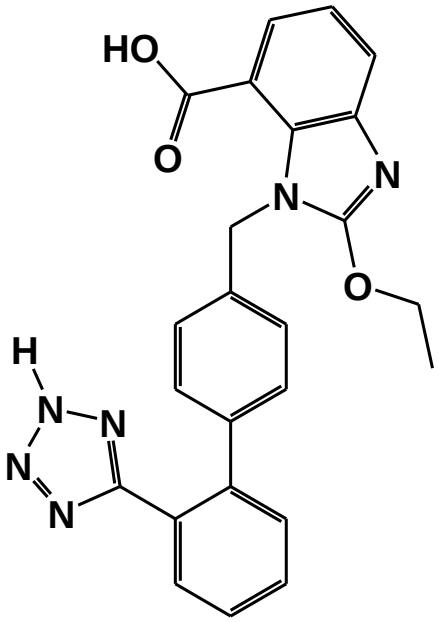

Scheme 1. Chemical Structure of Candesartan cilexetil

Silicon carbide (SiC) is obtained from the reduction of silica with a carbon containing source. Silicon carbide is the most common lapping powder. It can be used for almost all the materials. In this work, a new electrochemical method is introduced for determination of CAC. In which, continuous coulometric FFT cyclic voltammetry (CCFFTCV) technique [13-28] combined with a new sensor was used for sensitive detection of CAC. The sensor was designed based on fabrication of SiC nanoparticles and graphene nanosheets (GNS) hybrid mixed with ionic liquid, 1-Butyl-3-methylimidazolium hexafluoro-phosphate ([bmim][PF_6]) on a glassy carbon electrode. As one of the most important thing in this procedure, SiC NPs and GNS could act as a promising immobilization carrier for the detection owing to its unusual properties including high conductivity. Ionic liquid (IL) [bmim][PF_6] is a water-miscible (hydrophilic), which can form a film on glassy carbon electrodes with active electrochemical properties. Also, the presence of SiC NPs and GNS in modification of the electrode provides an environment, which enhances the electrocatalytic activities. Scanning electron microscopy and impedance spectroscopy (EIS) was used to characterize the electrode surface. Under optimal conditions, the proposed sensor exhibited a linear response to a wide concentration rage of CAC.

2. MATERIALS AND METHODS

2.1. Reagents

CAC, potassium ferricyanide, sodium chloride, potassium chloride, sodium phosphate dibasic (Na_2HPO_4) and sulfuric acid (98%), ethanol (98%) were all purchased form Merck Co. 1-Butyl-3-methylimidazolium hexafluorophosphate ([bmim][PF_6]) was purchased from Merck. Graphene nanosheets (GNS) and SiC powders with average particle size of 10-25 nm, were supplied by a local company in Iran. 0.05 M NaH_2PO_4/Na_2HPO_4 buffer solutions at pH 4.0 were used as the supporting electrolyte. The prepared solutions were kept at 4 °C before use.

2.2. The electrode preparation

A glassy carbon electrode, GCE, (3 mm in diameter) were polished well with 1.0, 0.3 and 0.05 μm alumina slurry and then it was washed thoroughly with doubly distilled water. The electrodes were successively sonicated in 1:1 nitric acid, acetone and doubly distilled water, and then allowed to dry at room temperature. Then 40 μl of EtOH–SiC solutions (0.1 to 1 mg/ml) was cast on the surface of GCE. Then, for construction of IL-GNS/SiC/GCE, 0.2 to1.0 mg graphene was added to 0.2 to 1.0 mg/mL IL and mixed together and ultrasonicated for 30 min. After that, 8.0 μL of IL-GNS mixture solution was cast on the surface of SiC and left it to dry at room temperature to form a stable film. The prepared sensor was stored at 4 °C in PBS before use. The schematic diagram of the construction of CAC sensor is shown in Fig. 1.

2.3. Instrumentation and Data Acquisition and Processing

For CCFFTCV voltammetric measurements a homemade potentiostat was used, which was connected to a PC. The computer equipped with an analog to digital data acquisition board (PCL-818H, Advantech Co.). Before each measurement, the three-electrode system was installed in a blank solution, and the peak current voltammetry scan from −700 to 200 mV (vs. SCE) was recorded. The EIS measurements were performed in 3 mM $K_3Fe(CN)_6$ in PBS at pH 4.0. A stock solution of 5 mM CAC was firstly prepared, and then an aliquot was diluted to the appropriate concentration.

In CCFFTCV method, the sensor response was calculated based on the charge under peak current in the recorded CVs. Therefore, the unit for the resulted response is change from ampere to coulomb (C).

The is the charge changes (ΔQ) under the CVs at a selected potential range, E_1 to E_2 calculated as follows,

$$\Delta Q_n = Q_n - Q_{ave} \quad \text{for n>0} \qquad (1)$$

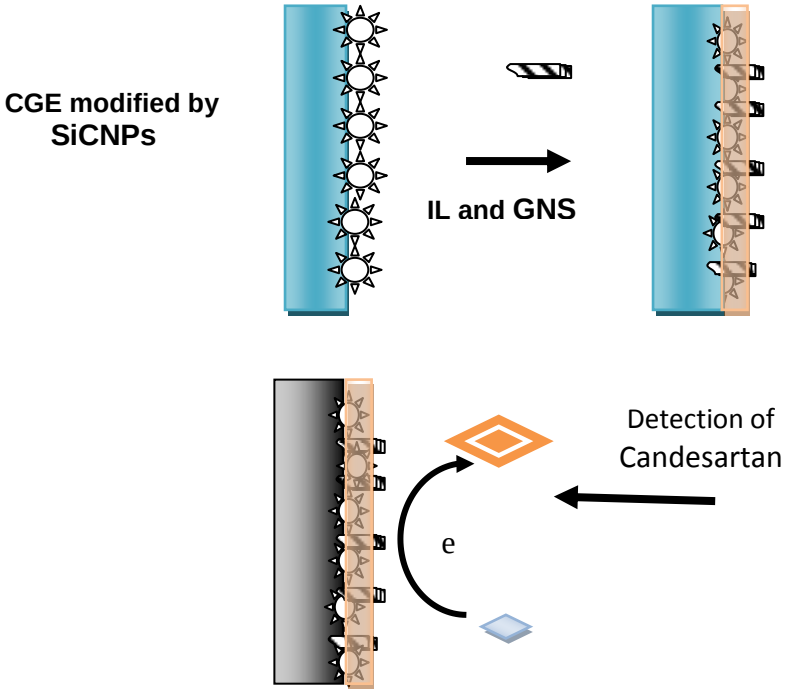

Figure 1. Schematic figures of the sensor preparation

or

$$\Delta Q_n = \int_{E_1}^{E_2} \Delta i_{(n,E)} dE - ave\left[\int_{E_1}^{E_2} \Delta i_{(m,E)} dE\right] \quad (2)$$

where Q_{ave} and are the calculated average charges at the selected potential range, E_1 to E_2, from $m=5$ CVs in absent of the analyte, Q_n the calculated charge at the same potential range from subsequent n^{th} cyclic voltammogram.

3. RESULTS AND DISCUSSION

Fig. 2A showed the CVs of CAC on the bear GCE (curve a) and IL-GNS/ SiC/GCE (curve b) 0.05 M phosphate buffer solution at pH 4.0 at scan rate 800 mV/s. As shown, a low redox activity is observed at the unmodified GC electrode over the applied potential range. The figure demonstrates a very weak cathodic, which is an indication of the weaker adsorption reaction of CAC species on the sensor surface. Conversely, for IL-GNS/ SiC/GC electrode, there is a well-defined cathodic peak on the modified electrode, in which anodic a peak potential is about -420 mV. It seems that the modified electrode demonstrates a significant reduction current in the forward scan and a very low oxidation signal in the reverse scan. This indicates that the electrochemical process is amplified by the modified

electrode. Moreover, observing a positive shift in the cathodic peak potential and remarkable increase of current is an indication of considerable catalytic ability of SiC NPs and GNS to reduction of CAC. It can suggest that IL-GNS/SiC can improve the electron-transfer rate and as well as, enhancing accumulation CAC molecules.

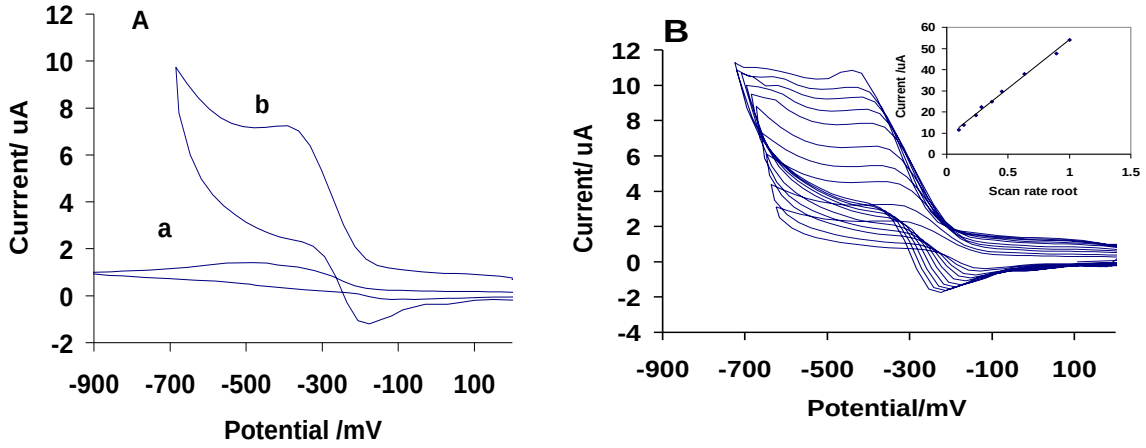

Figure 2. A) Cyclic voltammograms of 1 μM CAC in 0.05 M BPS pH 4.0 on (a) the bare GCE at scan rate 800 mV/s,(b) IL-GNS/SiC/GC electrode; B) Typical Cyclic voltammograms at different scan rates, 0.05, 0.1,0.2. 0.4 0.6 ,0.8, 1.5, 2.0, V/s. The inset shows plots of the cathodic peak current against the root of scan rate ν.

Also existing a lager surface area or conductive surface of the electrode provide more easily penetrates and adsorption CAC molecules. It is well know that the conductance of IL is higher at surface due to exist a low interfacial tension. This also can enhance current, as well as, the sensitivity of the sensor. This is reasonable to deduce that IL played an important role here.

CVs of CAC 1 μM on IL-GNS/ SiC/GCE with different scan rates range from 0.05 to 2.0V/s in PBS (pH 4.0) were shown in Fig. 2B. It can be noticed that with the step up of the scan rate, the current of the reduction peak increases linearly, with the linear egression equations as i_p = $4.5137v^{1/2}$ +8.921 (R = 0.988). Based on this result, it can be suggested that the reaction is diffusion-controlled behavior with an electron transfer process.

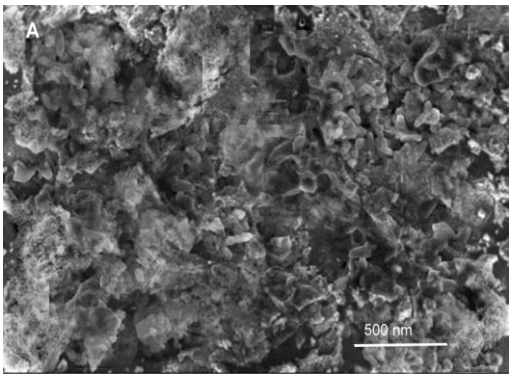

Figure 3. SEM images of the surface of IL-GNS/ SiC /GCE

Fig. 3 shows SEM image of the surface of the constructed IL-GNS/ SiC /GCE. In this figure, it could be seen that GNS showed the typical crumpled structure, and the magnitude and distribution of SiC on the surface. In fact, the composite surface is well-coated with GNS the diameters 20–90 nm.

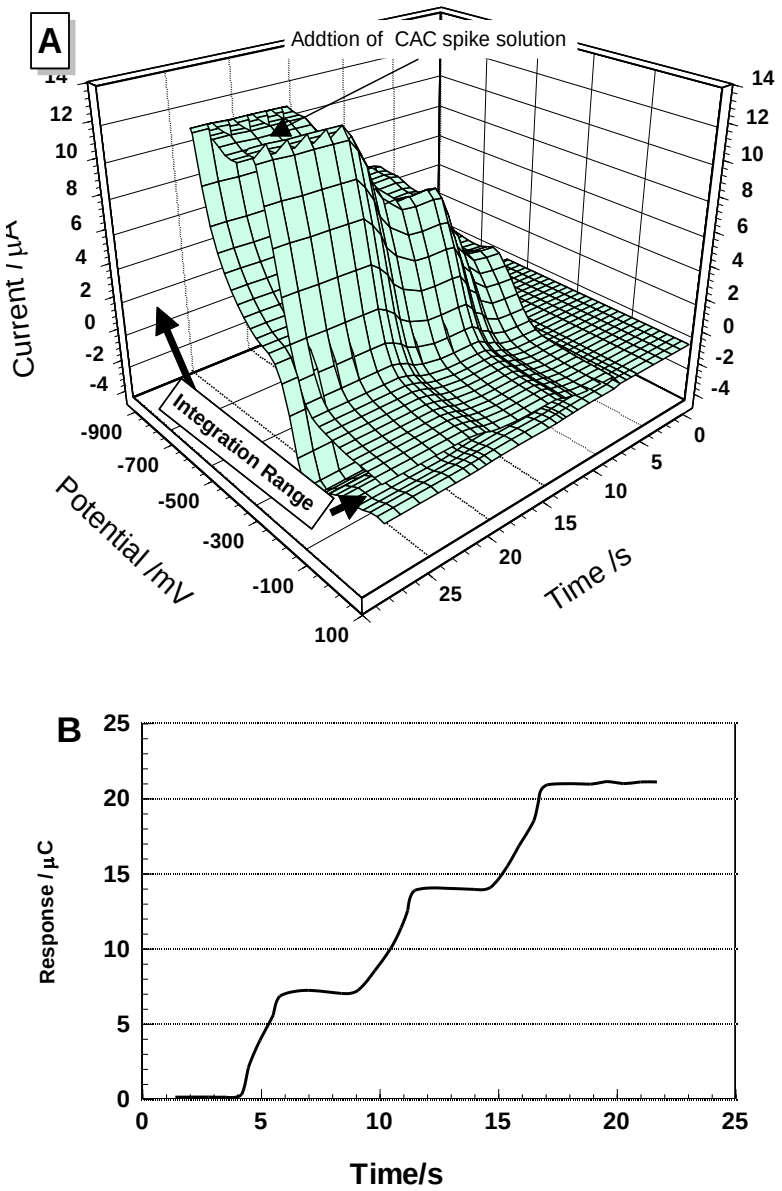

Figure 4. A) CCFFTCV voltammograms of the in absent and spiking of three standard solutions of 1×10^{-6} M CAC in PB solution at pH4.0. The potential range was of 100 to-700 mV at potential scan rate 2V/s. B) The calculated response for sensor in integral range of 100 to -700

Fig. 4A shows CCFFTCV voltammogramms and the changes in voltammetric of IL-GNS/SiC /GCE in the potential range of 100 to -700 mV in 0.05 M PB solution at pH 4.0, and at scan rate of 2 V/s. In this graph, the time axis represents the time window of the experiment, which is the time of applying CCFFTCV method on the sensor [14-17].

The figure shows that there is no notable current for the sensor in absent of CAC, but after spiking of 1.0×10^{-6} M CAC in the PBS a considerable response current appears at potential -490 mV. However, as mentioned above the accumulation of CAC on the high surface area of the sensor can enhance the peak current. As shown in equations 1 and 2, the electrode response, ΔQ, was calculated in form the integration of the currents in range of 100 to -700 mV (see Fig 4B). To get the best performance of the detector, the effect the most important experimental parameters were examined and optimized.

3.1. Optimization of sensor parameters

Due to this fact that the sensitivity of the CCFFTCV detection system mainly depends on the potential scan rate, it is needed to optimize the scan rate. From this point of view, the response of the sensor for solution of in 3.0×10^{-6} M CAC was tested at the potential scan rate of 0.5 to 5 V/s. As it is clear from the results demonstrated in Fig. 4, the detector exhibits the maximum sensitivity at scan rate 2 V/s. The effects of the scan rate on the sensor response or the detection performance could be taken into consideration from the limitations in the kinetic factor aspect of the electrochemical processes. Because at very high scan rates the response of the sensor declines.

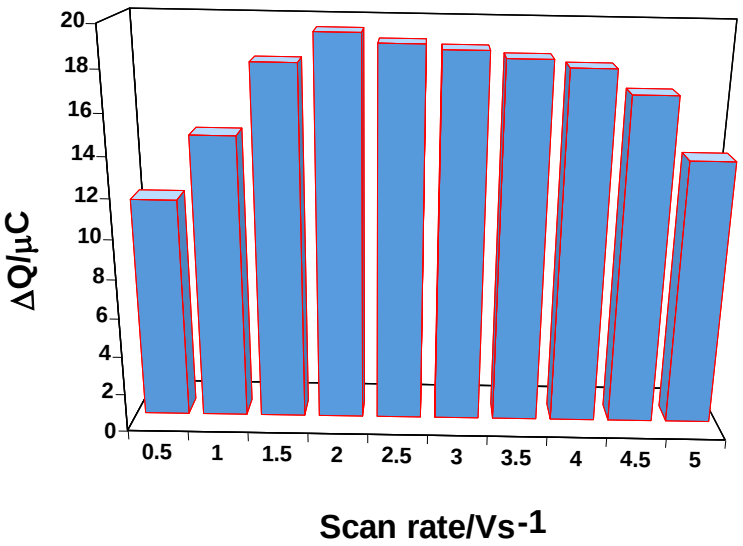

Figure 5. The effect of the sweep rate on the response of the modified GCE in 3.0×10^{-6} M, The potential range was of 100 to-700 mV at potential scan rate 2V/s. B)The calculated response for sensor in integral range of 100 to -700

The dependence of the electrochemical method on the solution pH was studied over the range pH 2.0 to 8.0. Fig. 5 shows the changes of ΔQ (or the sensor response) at scan rate of 2 V/s was subjected to 1 μM CAC solution at various pHs. The results showed that at the pH values less than 4.0, the peak current increase smoothly with the solution pH, up to pH 4.0. After that, at higher pHs the

response decreased. Nevertheless, form the graph, it can be concluded the best pH for the sensor operation is around 4.0

Also, the results show that, the peak potentials and current were dependent on pH values of the solution. It can be observed that the peak potentials for reduction is negatively shifted with increasing pH values. A plot of Ep vs. pH values shows straight lines at different pH range (see the inset in Fig. 6).

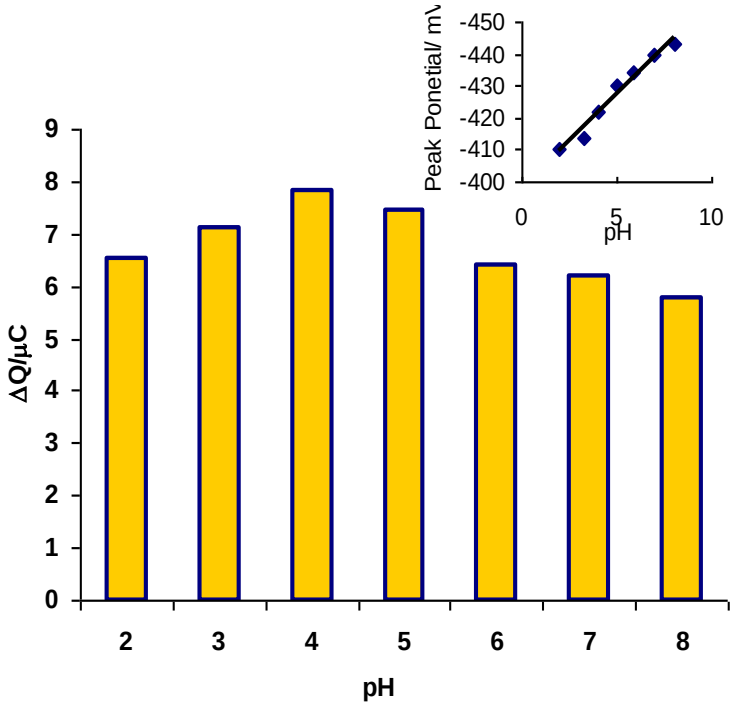

Figure 6. The effect of pH concentration on sensor response to 1.0×10^{-6} M CAC, in 0.05 M PB solution. The potential range of -700 to 100 mV at potential scan rate 2 V/s, the inset effect of pH on peak potential.

It is well known that amount of SiC NPs and GNS, could have a signification efect on the performance of the sensor. The relationship between the weights of SiC NPs and GNS in the modifier composition was investigated, where constant volumes of the nanoparticles solutions were casted on the electrode surface. Fig 6 shows the dependence of the response sensor to weights of GNS and SiC tested in 8×10^{-7} M CAC in 0.05 M PBS at pH 4.0 . As shown in figure, the value of ΔQ increase with weight of GNS to up to 6 mg the sensor response set at the maximum value. Whiles, at the higher weights of GNS the value of ΔQ decreases, which could be due to enhancement of resistance of the modifier. This may, also, reduce the effect of SiC NPs in conductivity of the surface.

Moreover, the change in the sensor sensitivity with the amount

of SiC Nps to the content of the modifier on the electrode surface was investigated. As shown in the figure the sensor response initially increases with weight of SiC, up to 0.7 mg and after that the response slightly decreases. Therefore, the optimum weight for SiC Nps was 0.8 mg.

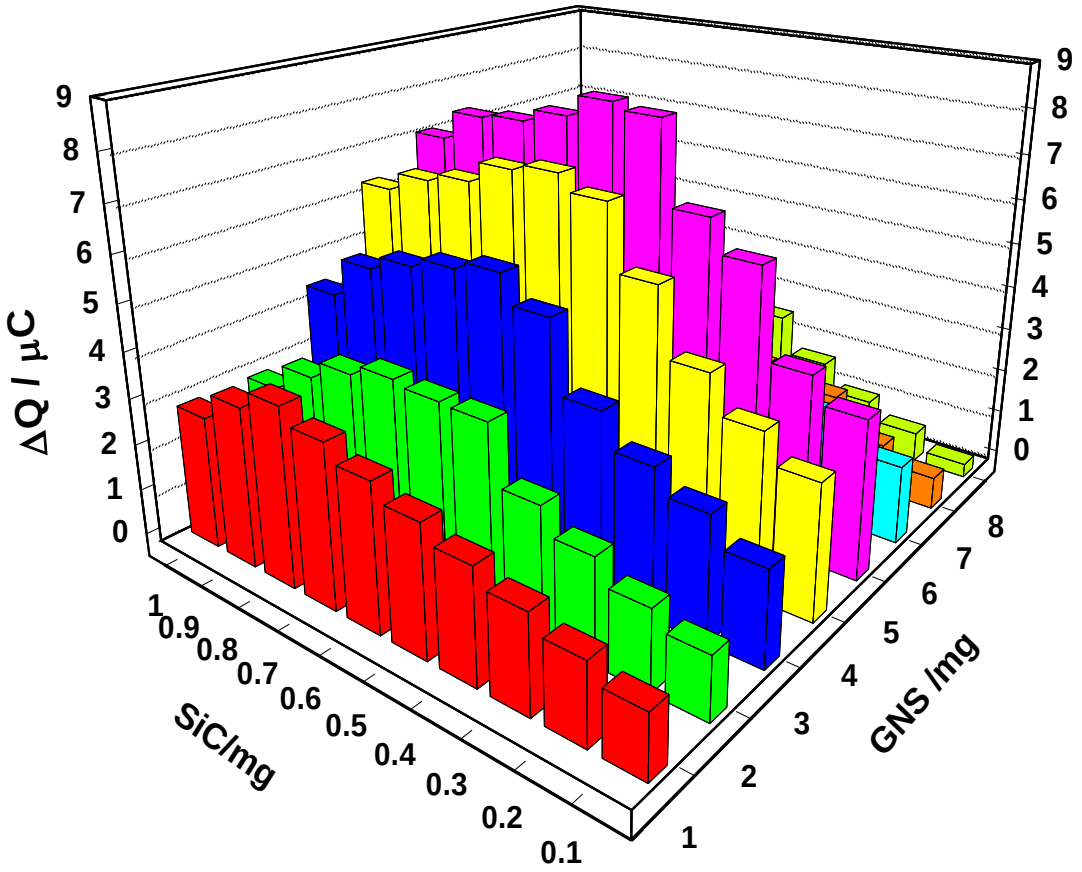

Figure 7. The effect of amount of GNS and SiC the on the response to 8.0×10^{-7} M of CAC he potential range of -700 to 100 mV at potential scan rate 2 V/s,in 0. 05 M PB solution at pH=4.0

3.2. Calibration curve

Fig. 7 shows the result of measurements of CAC standard solutions by CCFFTCV method under the optimized conditions. As mentioned above the sensor response to CAC sample solution was in μC. For this reason, the magnitude of the sensor response depends on the choice of the potential integration range in the CCFFTCV measurements. In this figure, each point represents the integrated signal for 3 consecutive additions of the CAC standard solution. A linear response of CAC reduction peak current as a function of CAC concentration (ΔQ (μC) = 5.070) was obtained in the range of 0.5×10^{-8} to 9.2×10^{-7} M, with a correlation coefficient (R) of 0.995 (insert Fig. 7). A detection limit (DL) of 5.2×10^{-9} M was obtained by using the relations 3Sb/b and 10Sb/b, where Sb is the blank standard deviation and b the slope of the calibration curve [20-24].

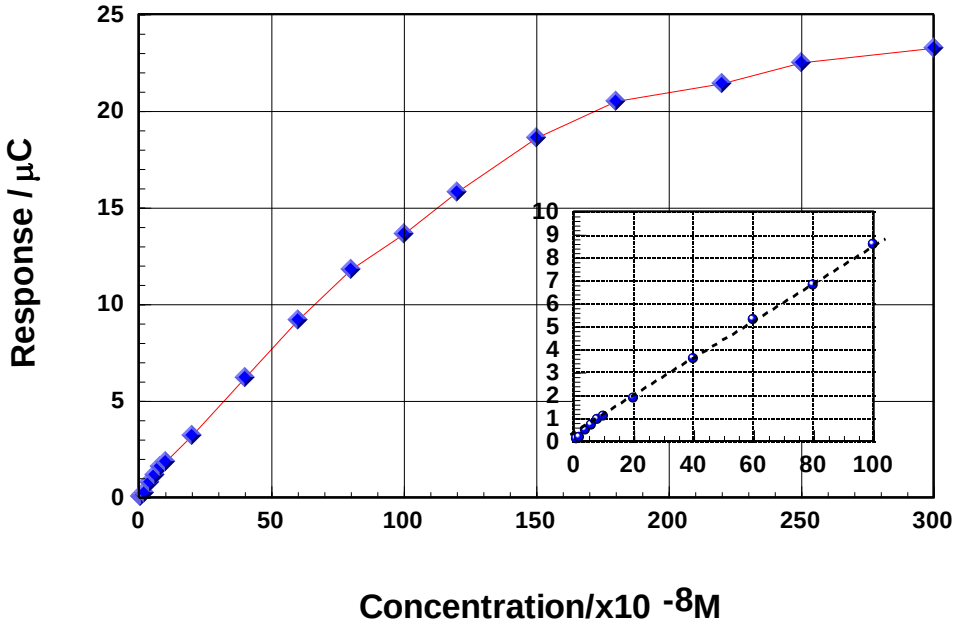

Figure 8. The calibration curve for CAC determination, the inset, response of the sensor to CAC PB solution, pH4.0 at potential scan rate 2 V/s. The potential range was of 100 to-700 mV at potential scan rate 2V/s. B)The calculated response for sensor in integral range of 100 to -700.

The long-term storage stability of the sensor was tested for 60 days. The sensitivity retained 98.4% of initial sensitivity up to 55 days. It was gradually decline, which might be due to the loss of the catalytic activity or adsorption of impurities on the electrode surface. In final evaluation, it was confirmed that the presented GNS and SiC NPs based CAC sensor combine with CCFFTCV exhibited an excellent and reproducible sensitivity.

4. CONCLUSIONS

This paper presents a highly sensitive electrochemical detection method for determination of CAC. The sensor was fabricated by modifying a GC electrode surface with silicon carbide nanoparticles on graphene nanosheets hybrid with ionic liquid (1-Butyl-3-methylimidazolium hexafluorophosphate ([bmim][PF_6]). The ionic liquid [bmim][PF_6] assembled on the sensor is not only responsible for a better immobilization of the NPs, but was also found to largely enhance current. The system was found well suited for the use of coulometric measurements as an excellent sensing system for CAC, with the advantage of overcoming the intrinsic problem of the overpotentials associated with the amperometic methods. The observed high sensitivity, long-term stability up to 60 days, and much lower limit of detection of the proposed nanosensor relative to the reported coulometric sensors in the literature clearly revealed that the nanocomposite used not only resulted in facilitated communication between CAC and the NPs, but also provided a proper microenvironment for electron transfer.

ACKNOWLEDGMENT
The authors express their appreciation to the Research Council of University of Tehran for financial support of this work.

References

1. L. R. Erhardt, *Int. J. Clin. Pract.* 59 (2005) 571.
2. S. Hillaert, T. R. M. De Beer, J. O. De Beer, W. Van den Bossche, W. *J. Chromatogr. A* 984 (2003)135.
3. T. Unger, *Am. J. Cardiol.* 84 (1999) 9S.
4. B. Michel, *Circulation* 103 (2001) 904.
5. T. L. Ripley, J. S. Chonlahan, R. E. Germany, *Clin. Interv. Aging* 1 (2006) 357.
6. H. Stenhoff, P. O. Lagerstrom, C. Andersen, *J. Chromatogr. B* 731 (1999) 411.
7. N. Ferreiros, S. Dresen, R. M. Alonso, W. Weinmann, *Drug Monit.* 29 (2007) 824.
8. M. Levi, G. Wuerzner, E. Ezan, A. Pruvost, *J. Chromatogr. B* 877 (2009) 919.
9. N. Erk, *Pharmazie* 58 (2003) 796.
10. B. Dogan, B. Uslu; S. A. Ozkan; *Pharmazie* 59 (2004) 841.
11. N. Maleki, G. Absalan, A. Safavi, and E. Farjami, *Anal. Chim. Acta*, 581 (2007) 37.
12. G. Y. Kim, A. Mulchandani, and W. Chen, *Anal. Biochem.*, 322 (2003) 251
13. P. Norouzi, H. Rashedi, T. Mirzaei Garakani, R. Mirshafian and M. R. Ganjali, *Int. J. Electrochem. Sci.* 5 (2010) 377.
14. P. Norouzi, M. R. Ganjali, B. Larijani, A. Mirabi-Semnakolaii, F. S. Mirnaghi, and A. Mohammadi, *Pharmazie* 63 (2008) 633.
15. P. Norouzi, M. R. Ganjali, S. Shirvani-Arani, and A. Mohammadi, *J. Pharm. Sci.* 95 (2007) 893.
16. M. R. Pourjavid, P. Norouzi, and M. R. Ganjali, *Int. J. Electrochem. Sci.* 4 (2009) 923.
17. P. Norouzi, M. R. Ganjali, M. Zare, and A. Mohammadi, *J. Pharm. Sci.* 96 (2007) 2009.
18. P. Norouzi, M. Qomi, A. Nemati, and M. R. Ganjali, *Int. J. Electrochem Sci.* 4 (2009) 1248.
19. P. Norouzi, B. Larijani, M. Ezoddin and M. R. Ganjali, *Mater. Sci. Eng. C* 28 (2008) 87.
20. M. R. Ganjali, P. Norouzi, R. Dinarvand, R. Farrokhi, and A. A. Moosavi-Movahedi, *Mater. Sci. Eng. C* 28 (2008) 1311.
21. P. Norouzi, M. R. Ganjali, and L. Hajiaghababaei, *Anal. Lett.*, 39 (2006) 1941.
22. P. Norouzi, G. R. Nabi Bidhendi, M.R. Ganjali, A. Sepehri, M. Ghorbani, *Microchim. Acta*, 152 (2005) 123.
23. P. Norouzi, M. R. Ganjali, T. Alizadeh, and P. Daneshgar, *Electroanalysis*, 18 (2006) 947.
24. M. R. Ganjali, P. Norouzi, M. Ghorbani, and A. Sepehri, *Talanta*, 66 (2005) 1225.
25. P. Norouzi, H. Ganjali, B. Larijani, F. Faridbod, M. R. Ganjali, and H. A. Zamani, *Int. J. Electrochem. Sci.* 6 (2011) 5189.
26. P. Norouzi, B. Larijani, F. Faridbod, M. R. Ganjali, *Int. J. Electrochem. Sci.* 5 (2010) 1550.
27. P. Norouzi, B. Larijani, and M. R. Ganjali, *Int. J. Electrochem. Sci.* 7 (2012) 7313.
28. P. Norouzi, F. Faridbod, H. Rashedi, and M. R. Ganjali, *Int. J. Electrochem. Sci.* 5 (2010) 1713.